

Utilization of brown seaweed adsorbent for effective removal of Pb(II) from wastewater: Biosorption and column studies

Hemavathi S¹, Kousalyadevi G^{2*}, Thiru S³ and Aravindan A⁴

¹Assistant Professor, Department of Civil Engineering, K Ramakrishnan College of Technology, Trichy - 621112, Tamilnadu, India.

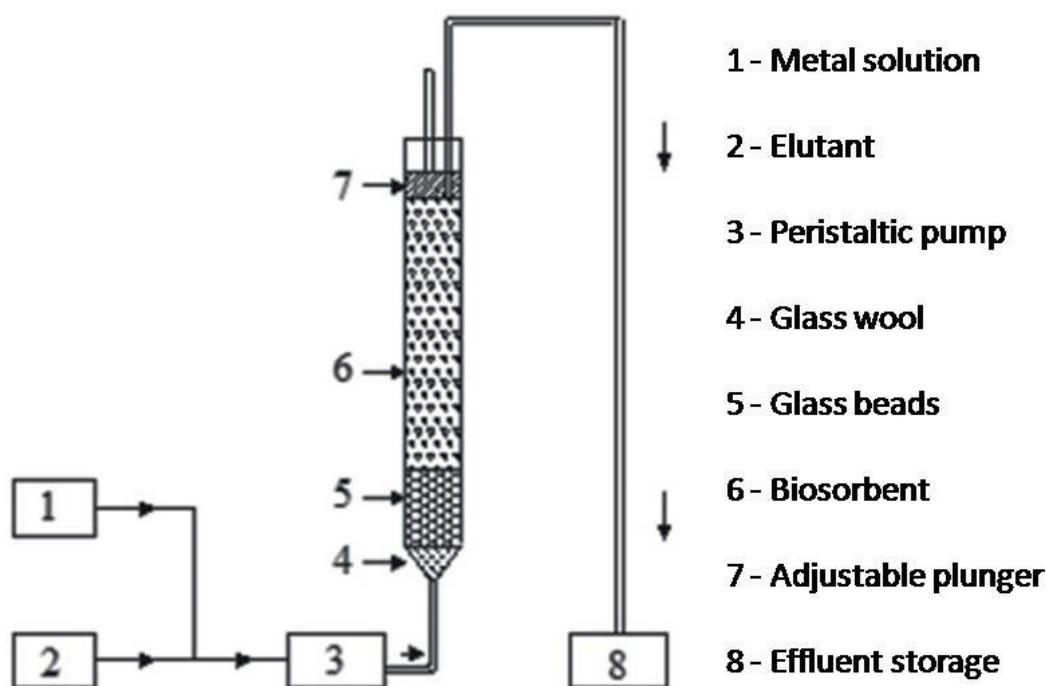
^{2*}School of Architecture and Interior Design, SRM Institute of Science and Technology, kattankulathur campus - 603203, Tamilnadu, India.

³Department of Mechanical and Materials Engineering, University of Jeddah, Jeddah - 21959, Kingdom of Saudi Arabia.

⁴Department of Civil Engineering, Koneru Lakshmaiah Educational Foundation, Guntur - 522502, Andhra Pradesh, India

*Corresponding Author Mail ID: kousym.arch@gmail.com

GRAPHICAL ABSTRACT



ABSTRACT

Researchers have been focusing on protecting water quality and preventing environmental contamination caused by industrial discharge of heavy metals. Various methods have been explored for extracting these metals from wastewater, but they often prove to be costly and rely on non-renewable resources. Adsorption, however, offers a promising solution due to its stability, affordability, and ease of implementation. In this research, continuous biosorption tests were conducted using a glass column filled with *Sargassum Wightii* (SW) seaweed, with Pb(II) ions used as a model solute. Varying bed heights (15-25cm) and flow rates (0.3-0.6 L/hr) in the column tests aimed to maximize biosorption efficiency. The optimal conditions for metal uptake and removal were a bed height of 25cm and a flow rate of 0.3L/hr, resulting in *Sargassum Wightii* adsorbing 41.17mg/g of metals with a removal efficiency of 69.07%. The Modified dose-response model effectively characterized Pb(II) biosorption at different bed heights and flow rates. Column regeneration studies demonstrated breakthrough and sorption within 2 hours, complete depletion at 24 hours, and an elution efficiency of 99.2% using 0.1M NaOH, allowing for up to three cycles of biosorbent reuse.

Keywords: Water quality; Biosorption; Heavy metals; Seaweed; Column studies

1 INTRODUCTION

Seaweeds are aquatic plants without true roots or stem, capable of autotrophic growth even in nutrient-limited conditions. Valued as biosorbents for size, sorption capacity, and safety. Studies by Trinelli *et al.* (2013), Abbas *et al.* (2014), and Shamim (2018) confirm this. Seaweeds are classified as micro, macro, and red seaweed, with brown seaweed being particularly effective at absorbing heavy metals. The attachment of metal ions to seaweed surfaces depends on species characteristics, metal charge, and solution composition.

In the aquatic environment, these plants are regarded as valuable renewable resources. India's seaweed floras are diverse, with tropical species predominating, but frigid, temperate, and subtropical species have also been documented. Too far, Indian seas have been home to approximately 271 genera and 1153 species of marine seaweed come in various shapes and types. Tamil Nadu currently ranks top regarding potential seaweed resources among the coastal states and union territories. *Sargassum* is large and rapidly growing tropical brown seaweed. While seaweed has industrial use, *Sargassum* organisms are particularly damaging in some regions of the world due to their extremely fast growth rate, flexible shape, and extraordinary vegetative renewal. As a result, the extra use of *S.wightii* is appealing and beneficial.

Lead is a toxic metal that accumulates in plants, organisms, and the human body. It exists in sulfide, cerussite, and galena forms. The primary source of lead pollution stems from industrial wastewater produced by sectors including electrical, steel, electroplating, and explosives. Its role

involves facilitating DNA and protein synthesis and ensuring cell replication. Adversely, it impairs the nervous system, kidneys, and mental well-being, and can induce cancer (Cechinel & de Souza, 2014). Plants and animals are both poisoned by lead. As a result, the most up-to-date approaches are needed to remove lead from water.

Table 1 assesses the adsorption capacity and efficiency of low-cost biosorbents (e.g., sawdust, leaves, fruit peels, crop waste, and biofertilizers) for removing Pb(II) metal ions from wastewater. It presents comparative results of their performance.

Table 1 Comparative review of Pb(II) sorption by the various adsorbent

Adsorbent	Sorbent Capacity (mg/g)	Adsorption Efficiency (%)	References
Raw rice bran	NA	40 to 50	Omar <i>et al.</i> 2020
Coir pith	NA	58	Bhattacharya <i>et al.</i> 2006
Coconut tree sawdust	NA	81	Rao <i>et al.</i> 2002
Banana pith	NA	100	Rao <i>et al.</i> 2002
<i>Gelidiella</i> species	NA	99.04	Seki <i>et al.</i> 1997
<i>Ensis siliqua</i>	0.79	5 to 40	Abia <i>et al.</i> 2003
Orange peel	1.078	NA	Ekpete <i>et al.</i> 1970
Sugarcane bagasse	1.7	90 to 95	Reddad <i>et al.</i> 2002
<i>Ulva</i> seaweed	2.43	15 to 20	Vázquez <i>et al.</i> 1994
Shells of almond	3.11	NA	Alshammari & Mutairah Shaker 2020
Coriander seed powder	3.331	70-80	Iqbal <i>et al.</i> 2009
Soybean hull	3.4	90 to 95	Reddad <i>et al.</i> 2002
Groundnut shells	3.83	51.4	Kaczala <i>et al.</i> 2009
Hardwood	4.54	NA	Chen <i>et al.</i> 2011
<i>Turbinaria</i> seaweed	4.86	15 to 20	Vázquez <i>et al.</i> 1994
Olive mill solid residue	5.4	NA	Gharaibeh <i>et al.</i> 1998
Banana peel	5.8	NA	Annadurai <i>et al.</i> 2003
<i>Padina australis</i>	7.01	90	Ahmaruzzaman 2011
Groundnut shell	7.62	24.61	Shukla & Pai 2005
<i>Sargassum glaucescens</i>	8.1	90	Ahmaruzzaman 2011
Peanut hulls	9	68	Brown <i>et al.</i> 2000
<i>Barbadensis</i> Miller leaves	10	60.2	Ademiluyi & Nze 2016
Teakwood sawdust	10.96	29.43	Shukla & Pai 2005

<i>Mucor rouxii</i>	11.09	90	Kweon <i>et al.</i> 2001
Peat moss	13.27	NA	Viraraghavan & Dronamraju 1993
Pecan shell	13.9	NA	Bansode <i>et al.</i> 2003
Walnut shell	13.92	96	Inyang <i>et al.</i> 2015
Leaves of <i>Tectona grandis</i> (teak wood)	16.42	High	Kumar <i>et al.</i> 2006
<i>Spirogyra insignis</i>	17.5	NA	Chen <i>et al.</i> 2011
Flax shive	18.2	NA	El-Shafey <i>et al.</i> 2002
Pigeon peas hulls	23.64	98.5	Mata <i>et al.</i> 2009
Mango peel	28.21	67.27	Iqbal <i>et al.</i> 2009
Bagasse AC	31.11	NA	Mohan & Singh 2002
Sesame straw biochar	34	100	Park <i>et al.</i> 2016
Meranti sawdust	35.97	94	Lu 2008
Rice bran	38.3	NA	Schiewer & Patil 2008
<i>Spirodela polyrhiza</i>	44.9	NA	Bogusz <i>et al.</i> 2015
<i>Sida hermaphrodita</i> biochar	48.08	NA	Bogusz <i>et al.</i> 2015
<i>Polyporous Versicolor</i>	57	NA	Marshall & Johns 1996
Soybean	69.8	NA	Schiewer & Patil 2008
Cottonseed hulls	72.8	NA	Schiewer & Patil 2008
Cassava waste (thioglycolic acid)	83.3	50	Horsfall <i>et al.</i> 2006
Wheat Straw	90.9	99.2	Janyasuthiwong <i>et al.</i> 2015
<i>Ulva</i> seaweed	173	10 to 15	Ademiluyi & David 2012
<i>Eucalyptus sheathiana</i> bark	250	69.38	Afroze <i>et al.</i> 2016
<i>Ceratophyllum demersum</i>	338.65	50	Horsfall <i>et al.</i> 2003

Heavy metals create highly hazardous health issues in the living tissues amongst the entire living beings due to incognizant intake of metals which exist in low concentration either through direct intake or the food chain. The effective removal of these heavy metal ions from the water bodies is an essential highlight in current research. Biosorption appears as a suitable process for the remediation of these heavy metals. The present study investigates the potential of seaweed *Sargassum Wightii* (Brown) biosorbent for heavy metal Lead (Pb). Initially, batch experiments are needed to perform to understand the optimum conditions and biosorption potential of a given biosorbent. A thorough understanding of sorption mechanisms is also required to replicate the process in real

conditions. Column experiments usually provide information regarding the applicability of the biosorbents in industrial applications and compactness with industrial effluents. Performing experiments in packed columns using best-performed biosorbent to simulate real industrial treatment processes. Optimizing the column process parameters (bed height, flow rate and starting metal concentration) for maximal metal removal. Using several models to analyze continuous sorption data.

2 MATERIALS AND METHODS

2.1 Biosorbent (Seaweed) and Chemicals

Sargassum Wightii (SW) seaweed from Kurusadai Island, Tamil Nadu, India, was collected, washed, air-dried, and finely chopped for sorption experiments. No chemical pretreatment was done. Analytical-grade chemicals from Sigma-Aldrich were used. The pH of the solution was adjusted with HCl or NaOH. A stock solution of Pb(II) at 1000 mg/L was prepared and diluted for the desired metal ion concentrations.

2.2 Analytical Instruments

Functional groups responsible for metal adsorption in the biosorbent were analyzed using the Perkin Elmer Spectrum RX1 Fourier IR spectrometer. Sample preparation involved KBr pellets. Scanning Electron Micrographs (SEM) and SEM-EDX analysis were performed using a JEOL JSM 6360 instrument. Pore characteristics were analyzed using the BET analyzer (AutosorbIQ Station 1). Metal ion concentrations were measured using AAS (Vario 6).

2.3 Column Experimental Procedure

2.3.1 Sorption

A packed bed column was used for continuous metal ion remediation. The column, made of acrylic glass, had dimensions of 33cm height and 1.9cm internal diameter. It contained a stainless sieve (0.05cm) and glass wool at the bottom, and a round bead (0.15cm diameter) placed 2cm above the bottom for flow uniformity. Figure 1 shows the schematic representation of the column.

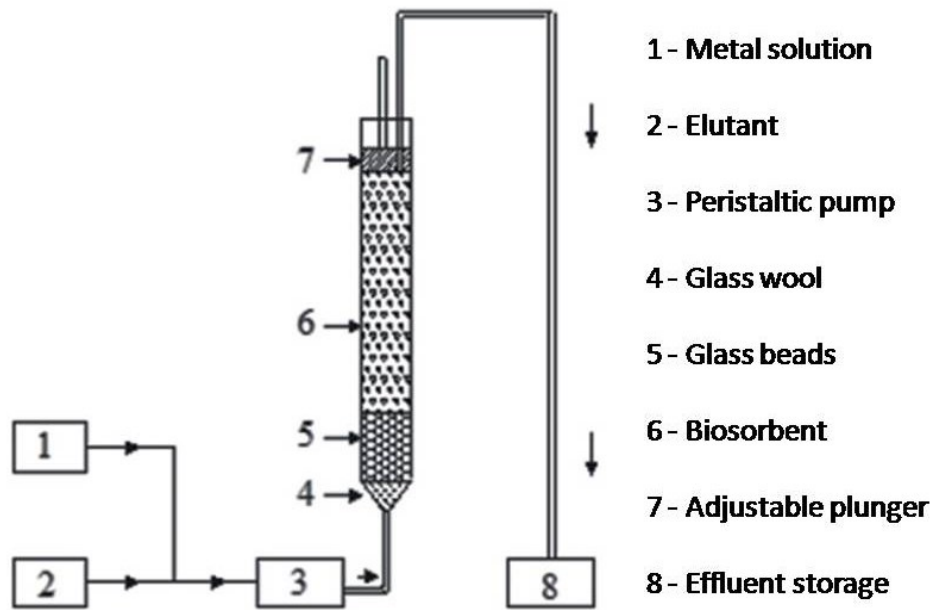


Figure 1 Schematic diagram of up-flow packed bed Column

2.3.2 Desorption

Desorption tests were performed to assess the biosorbent's durability for multiple elution cycles. The elutant, 0.1M NaOH, flowed at 0.3L/h. Periodic samples were collected from the top of the column and analyzed using an Atomic Absorption Spectrometer (AAS). Desorption was deemed complete when the metal concentration at the outlet reached 2% of the inlet concentration (2 mg/L).

2.3.3 Influence of Bed Height

Sorption experiments used different bed depths (15, 20, and 25cm) to study the impact of biosorbent sorption. The flow rate was constant at 0.3L/h, and the initial concentration of 100 mg/L was maintained.

2.3.4 Influence Rate of Flow

Different flow rates (0.3, 0.48, and 0.6L/h) were tested to examine their impact on metal ion sorption. The biosorbent bed depth and initial concentration of 100mg/L remained constant.

2.3.5 Influence of Initial Concentration of Metal

Different initial metal ion concentrations (50, 75, and 100 mg/L) were used to investigate their effect on biosorbent sorption. The optimal bed depth and flow rate were kept constant.

2.3.6 Column Data Analysis

Equations 1-5 calculated Δt , V_{eff} , m_{tot} , E , and total metal removal. Figure 1 showed the C/C_0 vs t plot, revealing the sorption mechanism in the packed column.

$$\Delta t = t_e - t_b \quad (1)$$

$$V_{eff} = F \cdot t_e \quad (2)$$

$$m_{tot} = \frac{C_0 \cdot F \cdot t_e}{1000} \quad (3)$$

$$Total\ metal\ removal(\%) = \frac{m_{adsor}}{m_{total}} \times 100 \quad (4)$$

$$E(\%) = \frac{m_{desor}}{m_{adsor}} \times 100 \quad (5)$$

where t_b - breakthrough time, t_e - bed exhaustion time, F - flow rate (L/h), C_0 - Initial concentration

2.3.7 Column Data Modeling

To explain the sorption modelling in the packed column in Figure 1, the following Equations 6 and 7 are used:

$$\text{Modified dose-response model: } \frac{C}{C_0} = 1 - \frac{1}{1 + \left(\frac{V_{eff}}{b_{mdr}} \right)^{a_{mdr}}} \quad (6)$$

$$\text{Yoon-Nelson model: } \frac{C}{C_0} = \frac{\exp(k_{YN}t - \tau k_{YN})}{1 + \exp(k_{YN}t - \tau k_{YN})} \quad (7)$$

The constants a_{mdr} and b_{mdr} represent the modified dose-response model, and k_{YN} represents the Yoon-Nelson model rate constant (min^{-1}). The parameter τ denotes the time for 50% breakthrough (min).

3 RESULTS AND DISCUSSION

3.1 Functional group spectra and surface analyses of *S.wightii*

FT-IR spectroscopy analysis played a crucial role in sorption studies by detecting changes in the frequency of sorbents and functional groups responsible for metal ion removal. The analysis focused on previously identified FT-IR spectroscopy peaks associated with different functional groups. Seaweed, specifically *S.wightii*, was examined for chemical classes such as carboxylic, amino, sulfonated, and hydroxyzine (Gokulan *et al.*, 2019(a)). Figure 2 displays the FT-IR spectra of raw seaweed and metal-loaded *S.wightii*. The raw seaweed exhibited multiple absorption peaks, indicating its dynamic nature. Specific peaks at certain wavenumbers represented various functional groups in the seaweed before adsorption. The presence of metal ions caused shifts in these wavenumbers, indicating the involvement of carboxylate biomass in metal binding. Significant changes were observed in the C=O and C-O stretches between metal-loaded *S.wightii* and the raw seaweed (Table 3). Moreover, significant changes in the symmetric and asymmetric-OSO₃ bands confirmed the presence of sulphonate groups compared to the raw *S.wightii* (Table 2). These findings indicated the presence of acidic groups (carboxyl and sulphonate) involved in binding heavy metal ions (Vijayaraghavan *et al.*, 2017).

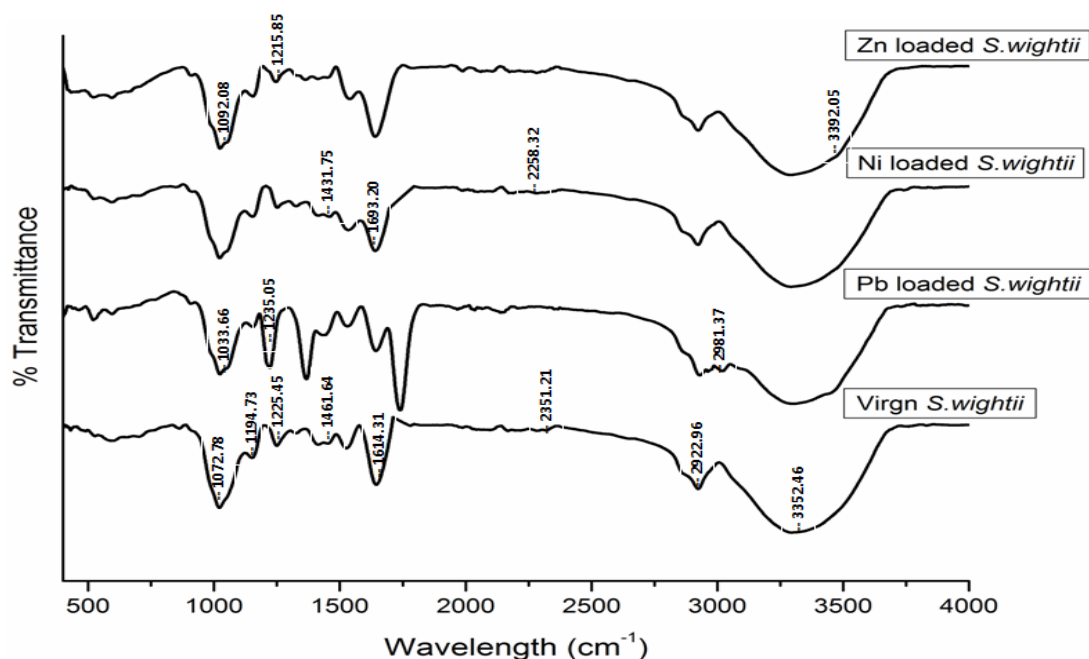


Figure 2 FT-IR spectra of raw and metal loaded *S.wightii*

Table 2 Stretching frequencies observed in raw and metal loaded *S.wightii*

Functional group	Wavenumber (cm ⁻¹)	
	Raw <i>S.wightii</i>	Pb loaded <i>S.wightii</i>
–OH, –NH stretching	3352.46	3362.16
Asymmetric CH ₂ stretching	2922.96	2981.37
–P–H– group	2351.21	2287.84
Asymmetric C=O stretch of COOH	1614.31	1614.31
Symmetric C=O	1461.64	1451.94
C–O (COOH) stretching	1225.45	1235.05
C=C stretching	1194.73	1145.91
C–O (alcohol) band	1072.78	1033.66

Figure 2 presents SEM images of untreated *S.wightii* and *S.wightii* loaded with Pb. The surface of untreated *S.wightii* exhibited crystalloid deposition protuberances and microstructures composed of sodium and other salt residues. In contrast, the surface of the seaweed appeared smooth after the biosorption of all tested metal ions. EDX analysis (Figure 2) was conducted to examine the samples. The raw seaweed showed high peaks of sodium (Na) and potassium (K), indicating their presence in seawater and uptake by the seaweed (Gokulan *et al.* 2019(b)). In the Pb-loaded *S.wightii* sample, distinct peaks corresponding to lead (Pb) were observed. Figure 3(b) showed a decrease in the frequency and disappearance of sodium (Na) peaks compared to the raw seaweed, indicating a

metal exchange mechanism. This suggests that captured metal ions replaced light metal ions during biosorption (Vijayaraghavan *et al.*, 2015). Similar results were observed for other metal ions in terms of the before/after adsorption mechanisms.

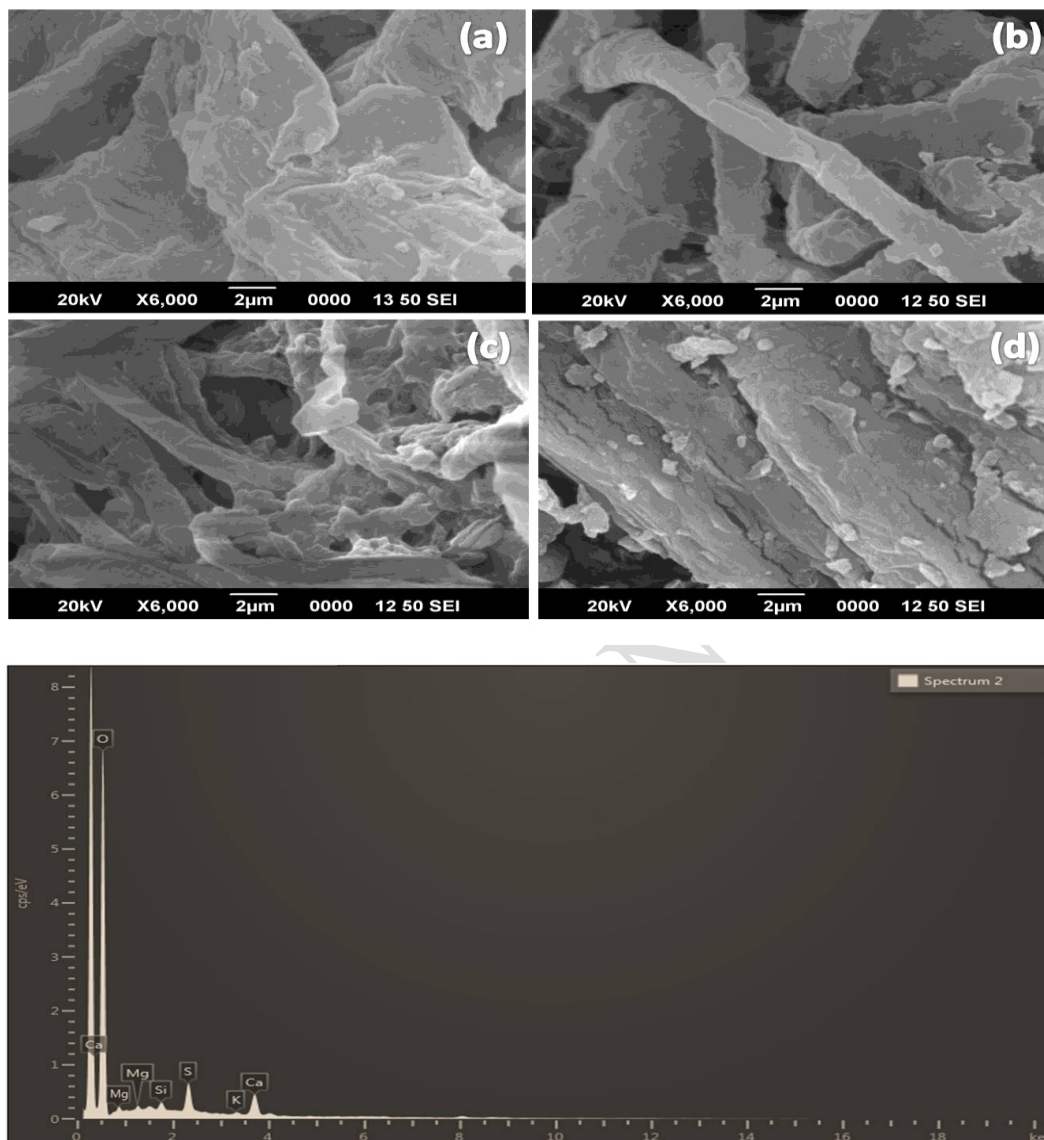


Figure 3 SEM EDX images of (a) raw *S.wightii* (b,c,d) Pb loaded *S.wightii*

3.2 Column Studies

The findings from the batch experiments aimed to understand the behaviour and performance of the biosorbent in metal biosorption. However, these results cannot be directly extrapolated to industrial treatment systems that operate on a continuous flow basis (Al-Sadat & Nezamzadeh, 2020). Consequently, column-based biosorption tests are necessary. A packed bed column is an effective approach for cyclic sorption-desorption processes in practical applications. This operational model ensures the maximum feasible concentration difference for driving metal biosorption. The saturated sorbent zone initiates at the inlet and gradually progresses along the column, eventually breakthrough occurring. The shape and slope of the breakthrough curve mainly depend on the equilibrium sorption isotherm and mass transport within the sorbent bed (Georgieva *et*

al., 2020). In the packed column tests, the most efficient seaweed (*S.wightii*) was employed for continuous Pb(II) removal. The initial metal concentration in all column studies was set at a modest 100 mg/L (in contrast to the batch experiments), as excessively high metal concentrations are uncommon in industrial effluents and yield gradual breakthrough curves.

3.2.1 Influence of Bed Height

Table 3 Column data and parameters obtained at different bed heights during biosorption of Pb(II) onto *S.wightii*

Metal	Bed height (cm)	Flow rate (L/hr)	Initial metal concentration (mg/L)	Uptake (mg/g)	t_b (h)	t_e (h)	Δt (h)	V_{eff} (L)	Total metal removal (%)
Pb(II)	15	0.3	100	40.9	2.75	11.75	9	3.52	68.47
	20	0.3	100	40.93	4.25	13.5	9.25	4.05	68.72
	25	0.3	100	41.17	5.5	15.5	10	4.65	69.07

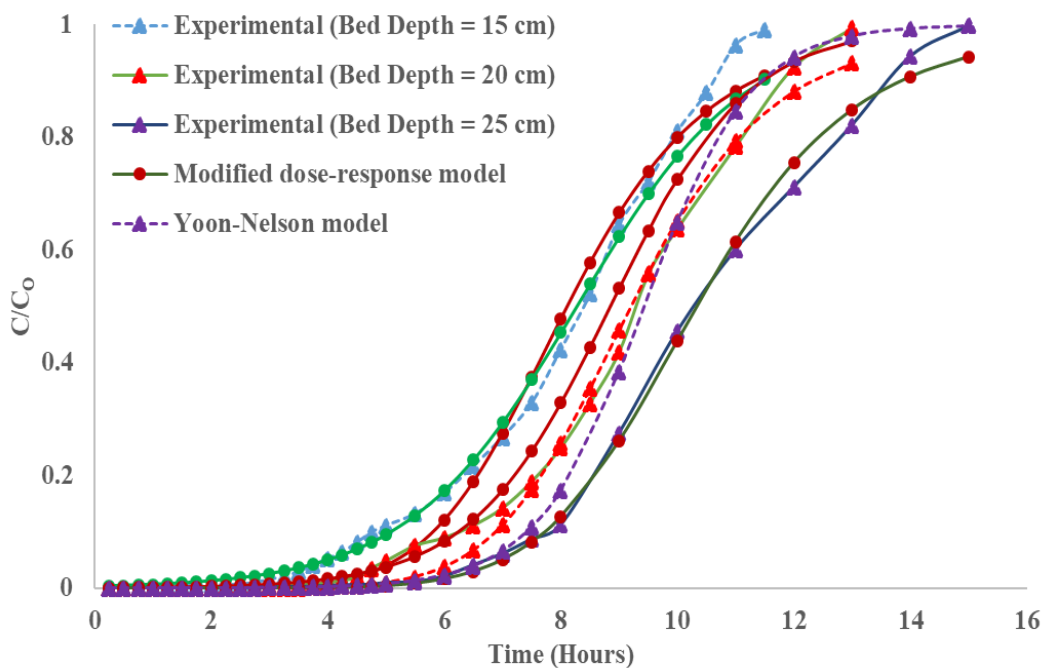


Figure 4 Effect of bed height during biosorption of Pb onto *S.wightii* in a continuous up-flow packed column (flow rate = 0.3 L/h; pH = 5; initial Pb concentration = 100 mg/L)

In continuous biosorption, bed depth affects metal adsorption. Trials at 15, 20, and 25cm bed depths with a flow rate of 0.3L/h and an initial metal concentration of 100mg/L were conducted. Biosorbent weights of 5.9, 6.8, and 7.8g achieved respective bed depths. Figure 4 shows breakthrough curves over time intervals. Adsorption capacities were 40.91, 40.93, and 41.18mg/g, with removal

efficiencies of 68.47, 68.72, and 69.07% for 15, 20, and 25cm depths. Maximum capacity and efficiency occurred at 25cm, with abundant binding sites favouring Pb(II) sorption (Venkatraman & Priya, 2021). Table 3 displays column parameters at different depths. The optimal bed depth was 25cm, with a treatment volume of 4.65L and a sorption zone of 10 hours.

3.2.2 Influence of Flow Rate

Table 4 Column data and parameters obtained at different flow rates during biosorption of Pb(II) onto *S.wightii*

Metal	Bed height (cm)	Flow rate (L/hr)	Initial metal concentration (mg/L)	Uptake (mg/g)	t_b (h)	t_e (h)	Δt (h)	V_{eff} (L)	Total metal removal (%)
Pb(II)	25	0.3	100	41.17	5.5	15.5	10	4.65	69.07
	25	0.48	100	37.58	3.25	9.5	6.25	4.56	64.29
	25	0.6	100	30.02	2	6.25	4.25	3.75	62.45

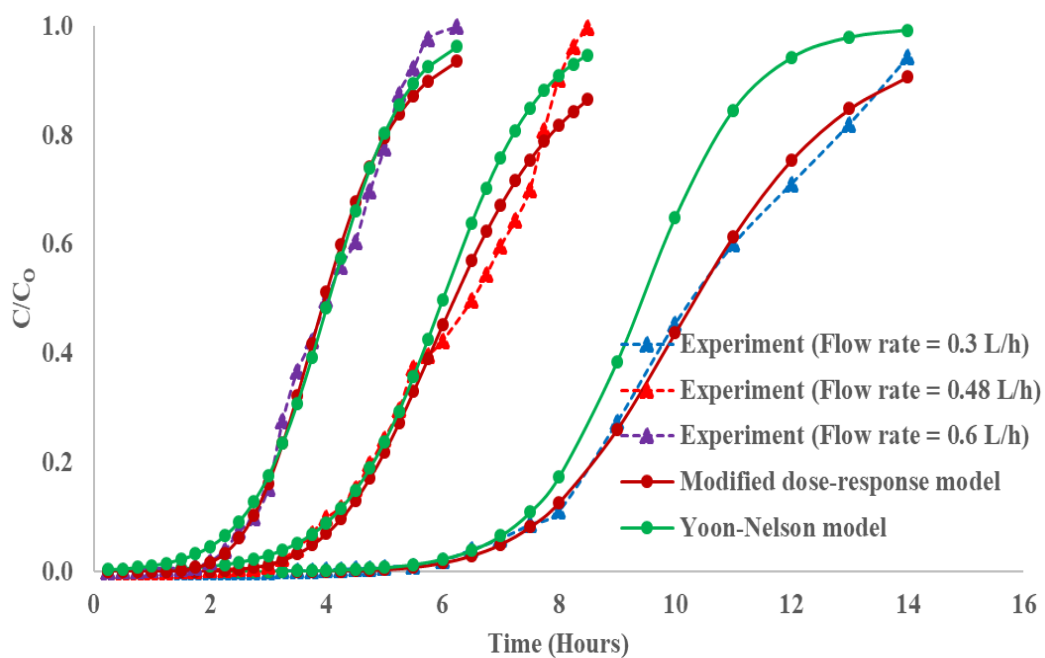


Figure 5 Effect of flow rate during biosorption of Pb onto *S.wightii* in a continuous up-flow packed column (bed height = 25cm; pH = 5; initial Pb concentration = 100 mg/L)

The impact of flow rate on industrial wastewater treatment was studied using flow rates of 0.3, 0.48, and 0.6L/h. Bed depth was 25cm, and initial Pb(II) concentration was 100mg/L. Table 4 summarizes column parameters at different flow rates, while Figure 5 shows breakthrough curves. Biosorbent absorbed 41.17, 37.58, and 30.02 mg/g, with elimination efficiencies of 69.07, 64.29, and

62.45% at 0.3, 0.48, and 0.6L/h, respectively. Higher flow rates led to earlier breakthroughs and shorter residence times. Lower flow rates allowed sufficient time for mass transfer, enhancing absorption and removal efficiencies. A flow rate of 0.3L/h maximized removal efficiency and absorption capacity (Karthik *et al.*, 2020; Pal *et al.*, 2021).

3.2.3 Influence of Initial Concentration of Pb(II)

Table 5 Column data and parameters obtained at different initial concentrations during biosorption of Pb(II) onto *S.wightii*

Metal	Bed height (cm)	Flow rate (L/hr)	Initial metal concentration (mg/L)	Uptake (mg/g)	t_b (h)	t_e (h)	Δt (h)	V_{eff} (L)	Total metal removal (%)
Pb(II)	25	0.3	100	41.17	5.5	15.5	10	4.65	69.07
	25	0.3	75	36.85	6.5	20	13.5	6	63.88
	25	0.3	50	34.89	9	29	20	8.7	62.56

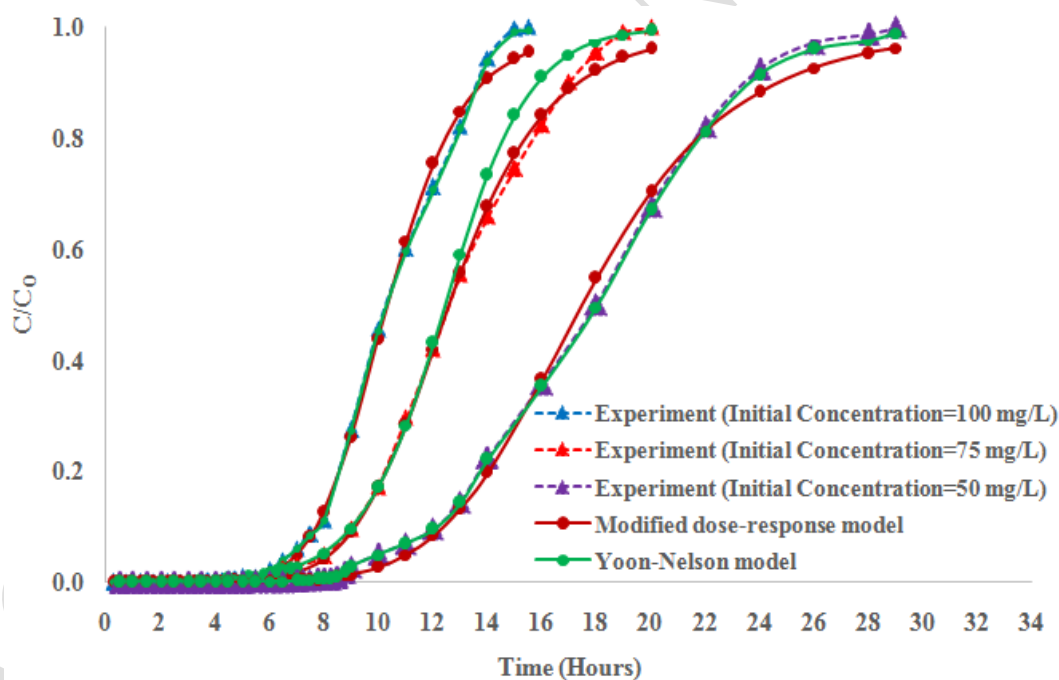


Figure 6 Effect of initial concentration during biosorption of Pb onto *S.wightii* in a continuous up-flow packed column (bed height = 25cm; pH = 5; flow rate = 0.3L/h)

Examined different initial concentrations (50, 75, and 100 mg/L) with constant flow rate and biosorbent depth of 0.3 L/h and 25 cm. Table 5 shows column parameters at various initial concentrations. Figure 6 depicts the impact of the initial Pb(II) concentration. Adsorption capacities were 41.18, 36.85, and 34.89 mg/g for 50, 75, and 100 mg/L, with removal efficiencies of 69.07%,

63.88%, and 62.56%. Lower initial concentrations offer more binding sites, leading to delayed breakthroughs, and lower operational characteristics (time, efficiency, uptake capacity) (El-Sayed *et al.*, 2019; Liu & Zhou *et al.*, 2021). The steepest breakthrough curve was observed at 100 mg/L, indicating the highest removal efficiency and smallest sorption zone.

3.2.4 Column Data Modeling

Table 6 Parameters predicted from Modified dose-response and Yoon-Nelson model during biosorption of Pb onto *S.wightii* at different bed heights

Bed height (cm)	Flow rate (L/hr)	Initial metal concentration (mg/L)	Modified dose-response model			Yoon-Nelson model		
			a _{mdr}	b _{mdr}	R ²	t	k _{YN}	R ²
15	0.3	100	6.5874	2.4315	0.9884	8.2711	0.6896	0.9841
20	0.3	100	7.5539	2.7612	0.9946	8.8466	0.8414	0.9608
25	0.3	100	7.5251	3.1006	0.9975	9.4307	1.0889	0.9934
25	0.48	100	5.9098	2.9743	0.9813	6.0065	1.1571	0.9866
25	0.6	100	5.8925	2.3798	0.9917	4.0445	1.4815	0.9937
25	0.3	75	6.8871	3.7710	0.9986	12.4321	0.6477	0.9978
25	0.3	50	6.3505	5.2369	0.9975	13.0581	0.9466	0.9129

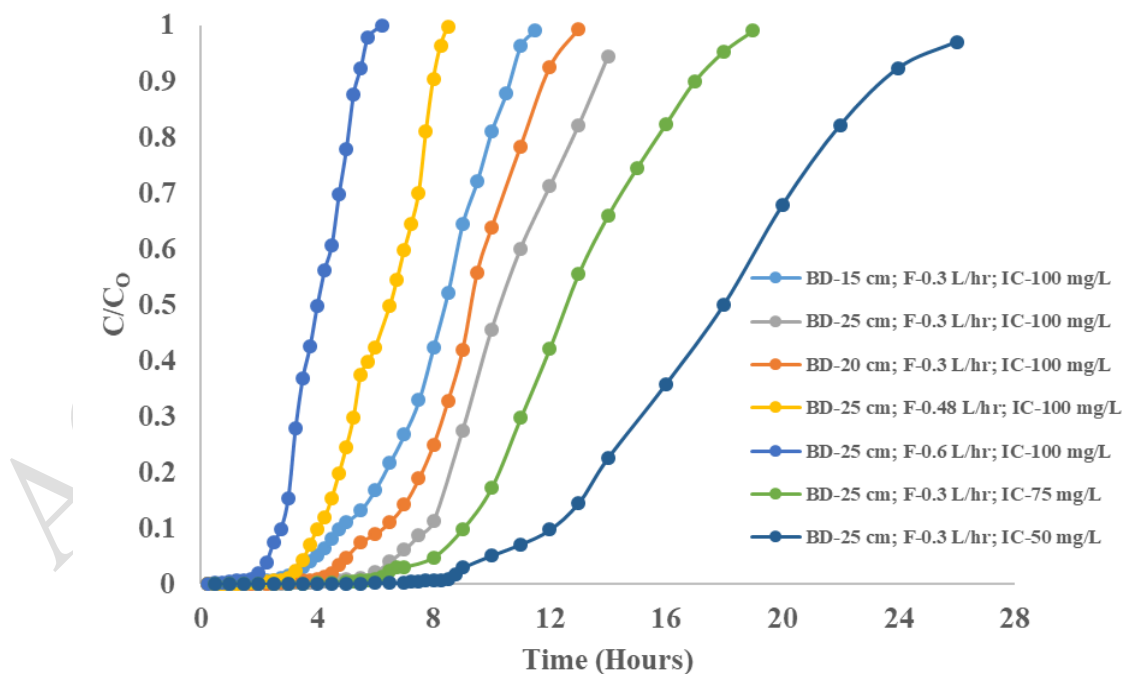


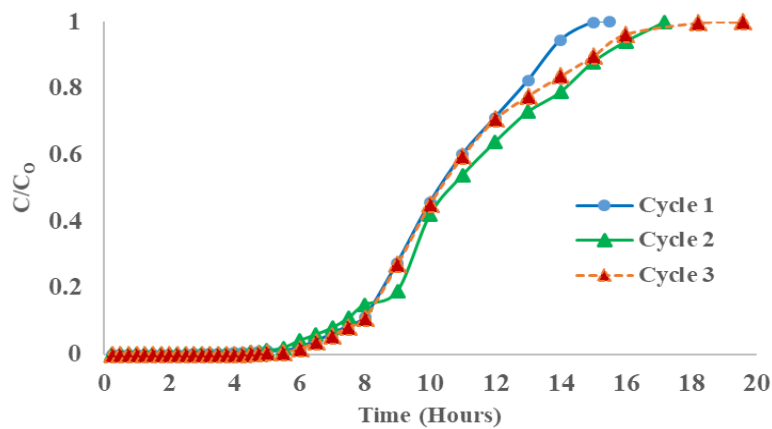
Figure 7 Modified dose-response and Yoon-Nelson model plot during biosorption of Pb onto *S.wightii* in a continuous up-flow packed column at different bed heights (Sorbent Depth (BD); Flowrate (F); Initial Concentration (IC) (flow rate = 0.3 L/h; pH = 5; initial Pb concentration = 100 mg/L).

Packed bed column used in wastewater treatment, and breakthrough curve predicted using mathematical models. Experimental data from Modified dose-response and Yoon-Nelson models were compared (Figure 7). The modified dose-response model was found most suitable. Table 6 shows model constants under different conditions. Underutilization of biosorbent's adsorption capacity at the highest rate constants may explain contrasting results. Yoon-Nelson model indicates a decrease in sorbate sorption rate linked to sorbate adsorption and breakthrough in column (Ozcan *et al.*, 2018). A modified dose-response model was developed to achieve a better fit based on previous research (Harsha *et al.*, 2020). The modified dose-response model outperformed the Yoon-Nelson model in terms of correlation coefficient R^2 and error analysis.

3.2.5 Column Regeneration

Table 7 Column data and parameters obtained at three sorption cycles during biosorption of Pb(II) onto *S.wightii*

Cycle	Bed height (cm)	Flow rate (L/h)	Initial metal concentration (mg/L)	Uptake (mg/g)	t_b (h)	t_e (h)	Δt (h)	V_{eff}	Total metal removal (%)
								(L)	
1	25	0.3	100	41.17	5.5	15.5	10	4.65	69.07
2	25	0.3	100	40.9	4	17.2	13.2	5.16	65.85
3	25	0.3	100	39.8	4.25	19.6	15.35	5.88	51.74



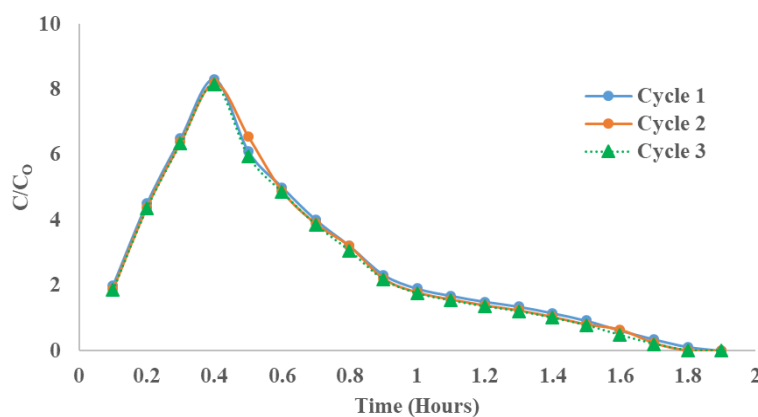


Figure 8 Column breakthrough and elution curve obtained during biosorption of Pb onto *S.wightii* in a continuous up-flow packed column (bed height = 25 cm; sorption flow rate = 0.3 L/h; pH = 5; initial Pb concentration = 100 mg/L; elutant = 0.1 M NaOH; elution flow rate = 10 mL/min)

To optimize cost-effective wastewater treatment, the regeneration capacity of the metal-bound sorbent is crucial. In sorption-elution cycles, a sorbent mass of 7.8g, bed depth of 25cm, and flow rate of 0.3L/h are employed. The quantity of metal bound to the sorbent is regenerated for subsequent sorption cycles. Table 8 lists the various column operating parameters during three regeneration cycles. Figures 8 depict the sorption and elution of Pb(II) across three sorption-elution cycles. Column breakthrough time was reduced and operation time increased as the regeneration trials progressed through consecutive cycles. As a result, the total sorption zone increased. The mass transfer zone expanded as cycles increased, but the removal effectiveness dropped (Abdelkader *et al.* 2021). The sorbent's uptake capacity remained consistent during the three sorption cycles, indicating that it may be used successfully for three sorption cycles (Table 7).

The decline in adsorption efficiency is due to functional group loss in the sorbent (Alalwan *et al.*, 2020). Elution lasted 2 hours, stopping at 2 mg/L effluent concentration. The breakthrough curve initially rose but then sharply dropped in all three elution cycles. In cycle 1, a high Pb(II) concentration of 8.3 times the initial concentration was observed at 24 minutes. Desorption efficiency surpassed 99.2% in all cycles, using a total volume of 5.88L of 0.1M NaOH as the eluent.

CONCLUSIONS

Biosorption of Pb(II) by *Sargassum Wightii* seaweed was found to be a feasible and effective method in this study. Column tests using a *Sargassum Wightii*-loaded packed column evaluated design elements and achieved optimal results with a bed height of 25 cm and flow rate of 0.3 L/hr, resulting in superior Pb(II) adsorption and elimination percentages. Modified dose-response and Yoon-Nelson models were used for data analysis, and metal adsorption reached 41.17 mg/g with a 69.07% removal rate at the optimal conditions. Regeneration experiments showed the reusability of

Sargassum Wightii with 0.1M NaOH, demonstrating sorption adsorption of 41.17 mg/g and desorption efficiency of 99.2%. These findings support the potential of seaweed biosorbents as cost-effective and eco-friendly alternatives to activated carbon for treating metal-bearing wastewater.

References

1. Abbas, SH, Ismail, IM, Mostafa, TM & Sulaymon, AH 2014, 'Biosorption of heavy metals: a review', *Journal of Chemical Science and Technology*, vol. 3, no. 4, pp. 74–102.
2. Abdelkader, SE, El-Gendy, AS & El-Haggar, S 2021, 'Removal of trivalent chromium from tannery wastewater using solid wastes', *Innovative Infrastructure Solutions*, vol. 6, no. 2, pp. 1–6.
3. Abia, AA, Horsfall, M & Didi, O 2003, 'The use of chemically modified and unmodified cassava waste for the removal of Cd, Cu and Zn ions from aqueous solution', *Bioresource Technology*, vol. 90, no. 3, pp. 345–348.
4. Ademiluyi, FT & David-West, EO 2012, 'Effect of Chemical Activation on the Adsorption of Heavy Metals Using Activated Carbons from Waste Materials', *ISRN Chemical Engineering*, vol. 05, pp. 1–5.
5. Ademiluyi, FT 2016, 'Multiple adsorption of heavy metal ions in aqueous solution using activated carbon from nigerian bamboo', *International Journal of Research in Engineering and Technology*, vol. 05, no. 01, pp. 164–169.
6. Afroze, S, Sen, TK & Ang, HM 2016, 'Adsorption removal of Zinc (II) from aqueous phase by raw and base modified *Eucalyptus sheathiana* bark: Kinetic, mechanism and equilibrium study', *Process Safety and Environmental Protection*, vol. 102, pp. 336–352.
7. Ahmaruzzaman, M 2011, 'Industrial wastes as low-cost potential adsorbents for the treatment of wastewater laden with heavy metals', *Advances in Colloid and Interface Science*, vol. 166, no. 1-2, pp. 36–59.
8. Alalwan, HA, Kadhom, MA & Alminshid, AH 2020, 'Removal of heavy metals from wastewater using agricultural byproducts', *Journal of Water Supply: Research and Technology-Aqua*, vol. 69, no. 2, pp. 99–112.
9. Al-Sadat Shafiof, M & Nezamzadeh-Ejhieh, A 2020, 'A comprehensive study on the removal of Cd(II) from aqueous solution on a novel pentetic acid-clinoptilolite nanoparticles adsorbent: Experimental design, kinetic and thermodynamic aspects', *Solid State Sciences*, vol. 99, pp. 106–110.
10. Alshammari, MS 2020, 'Assessment of Sewage Water Treatment Using Grinded Bauxite Rock as a Robust and Low-Cost Adsorption', *Journal of Chemistry*, vol. 02, pp. 1–5.

11. Annadurai, G, Juang, RS & Lee, DJ 2003, 'Adsorption of heavy metals from water using banana and orange peels', *Water Science and Technology*, vol. 47, no. 1, pp. 185–190.
12. Bansode, R, Losso, J, Marshall, W, Rao, R & Portier, R 2003, 'Adsorption of metal ions by pecan shell-based granular activated carbons', *Bioresource Technology*, vol. 89, no. 2, pp. 115–119.
13. Bhattacharya, AK, Mandal, SN & Das, SK 2006, 'Adsorption of Zn(II) from aqueous solution by using different adsorbents', *Chemical Engineering Journal*, vol. 123, no. 1-2, pp. 43–51.
14. Bogusz, A, Oleszczuk, P & Dobrowolski, R 2015, 'Application of laboratory prepared and commercially available biochars to adsorption of cadmium, copper and Zinc ions from water', *Bioresource Technology*, vol. 196, pp. 540–549.
15. Brown, P, Atly Jefcoat, I, Parrish, D, Gill, S & Graham, E 2000, 'Evaluation of the adsorptive capacity of peanut hull pellets for heavy metals in solution', *Advances in Environmental Research*, vol. 4, no. 1, pp. 19–29.
16. Cechinel, MAP, Mayer, DA, Pozdniakova, TA, Mazur, LP, Boaventura, RAR, de Souza, AAU & Vilar, VJP 2016, 'Removal of metal ions from a petrochemical wastewater using brown macro-seaweed as natural cation-exchangers', *Chemical Engineering Journal*, vol. 286, pp. 1–15.
17. Chen, X, Chen, G, Chen, L, Chen, Y, Lehmann, J, McBride, MB & Hay, AG 2011, 'Adsorption of copper and Zinc by biochars produced from pyrolysis of hardwood and corn straw in aqueous solution', *Bioresource Technology*, vol. 102, no. 19, pp. 8877–8884.
18. Ekpote, OA, Kpee, F, Amadi, JC & Rotimi, RB 1970, 'Adsorption of Chromium(VI) and Zinc(II) Ions on the Skin of Orange Peels (*Citrus sinensis*)', *Journal of Nepal Chemical Society*, vol. 26, pp. 31–39.
19. El-Sayed, WN, Elwakeel, KZ, Shahat, A & Awual, MR 2019, 'Investigation of novel nanomaterial for the removal of toxic substances from contaminated water', *RSC Advances*, vol. 9, no. 25, pp. 14167–14175.
20. El-Shafey, E, Cox, M, Pichugin, A & Appleton, Q 2002, 'Application of a carbon sorbent for the removal of cadmium and other heavy metal ions from aqueous solution', *Journal of Chemical Technology & Biotechnology*, vol. 77, no. 4, pp. 429–436.
21. Georgieva, VG, Gonsalvesh, L & Tavlieva, MP 2020, 'Thermodynamics and Kinetic of the removal of nickel (II) ions from aqueous solutions by biochar adsorbent made from agro-waste walnut shells', *Journal of Molecular Liquids*, vol. 312, pp. 112–118.
22. Gharaibeh, SH, Abu-el-sha'r, WY & Al-Kofahi, MM 1998, 'Removal of selected heavy metals from aqueous solutions using processed solid residue of olive mill products', *Water Research*, vol. 32, no. 2, pp. 498–502.

23. Gokulan, R, Avinash, A, Prabhu, GG & Jegan, J 2019, 'Remediation of remazol dyes by biochar derived from *Caulerpa scalpelliformis*—An eco-friendly approach', *Journal of Environmental Chemical Engineering*, vol. 7, no. 5, pp. 103–109.
24. Gokulan, R, Ganesh Prabhu, G & Jegan, J 2019, 'A novel sorbent *Ulva lactuca* -derived biochar for remediation of Remazol Brilliant Orange 3R in packed column', *Water Environment Research*, vol. 91, no. 7, pp. 642–649.
25. Gokulan, R, Prabhu, GG & Jegan, J 2019, 'Remediation of complex remazol effluent using biochar derived from green seaweed biomass', *International Journal of Phytoremediation*, vol. 21, no. 12, pp. 1179–1189.
26. Harsha Vardhan, K, Kumar, PS & Panda, RC 2020, 'Adsorption of copper ions from polluted water using biochar derived from waste renewable resources: static analysis', *International Journal of Environmental Analytical Chemistry*, vol. 102, no. 2, pp. 342–379.
27. Horsfall, M 2003, 'Sorption of cadmium(II) and Zinc(II) ions from aqueous solutions by cassava waste biomass (*Manihot sculenta* Cranz)', *Water Research*, vol. 37, no. 20, pp. 4913–4923.
28. Inyang, MI, Gao, B, Yao, Y, Xue, Y, Zimmerman, A, Mosa, A & Cao, X 2015, 'A review of biochar as a low-cost adsorbent for aqueous heavy metal removal', *Critical Reviews in Environmental Science and Technology*, vol. 46, no. 4, pp. 406–433.
29. Iqbal, M, Saeed, A & Kalim, I 2009, 'Characterization of Adsorptive Capacity and Investigation of Mechanism of Cu^{2+} , Ni^{2+} and Zn^{2+} Adsorption on Mango Peel Waste from Constituted Metal Solution and Genuine Electroplating Effluent', *Separation Science and Technology*, vol. 44, no. 15, pp. 3770–3791.
30. Janyasuthiwong, S, Phiri, SM, Kijjanapanich, P, Rene, ER, Esposito, G & Lens, PNL 2015, 'Copper, lead and Zinc removal from metal-contaminated wastewater by adsorption onto agricultural wastes', *Environmental Technology*, vol. 36, no. 24, pp. 3071–3083.
31. Kaczala, F, Marques, M & Hogland, W 2009, 'Lead and vanadium removal from a real industrial wastewater by gravitational settling/sedimentation and sorption onto *Pinus sylvestris* sawdust', *Bioresource Technology*, vol. 100, no. 1, pp. 235–243.
32. Karthik, V, Kumar, PS, Harsha Vardhan, K, Saravanan, K & Nithyakala, N 2020, 'Adsorptive behaviour of surface tailored fungal biomass for the elimination of toxic dye from wastewater', *International Journal of Environmental Analytical Chemistry*, vol. 102, no. 3, pp. 1–16.
33. Kumar, YP, King, P & Prasad, VSRK 2006, 'Zinc biosorption on *Tectona grandis* L.f. leaves biomass: Equilibrium and kinetic studies', *Chemical Engineering Journal*, vol. 124, no. 1, pp. 63–70.

34. Kweon, DK, Choi, JK, Kim, EK & Lim, ST 2001, 'Adsorption of divalent metal ions by succinylated and oxidized corn starches', *Carbohydrate Polymers*, vol. 46, no. 2, pp. 171–177.
35. Liu, D & Zhou, S 2021, 'Application of chemical coagulation to phosphorus removal from glyphosate wastewater', *International Journal of Environmental Science and Technology*, vol. 19, pp. 2345–2352.
36. Lu, X 2008, 'Thermodynamic and isotherm studies of the biosorption of Cu(II), Pb(II), and Zn(II) by leaves of saltbush (*Atriplex canescens*)', *The Journal of Chemical Thermodynamics*, vol. 40, no. 4, pp. 739–740.
37. Marshall, WE & Johns, MM 1996, 'Agricultural By-products as Metal Adsorbents: Sorption Properties and Resistance to Mechanical Abrasion', *Journal of Chemical Technology & Biotechnology*, vol. 66, no. 2, pp. 192–198.
38. Mata, YN, Blázquez, ML, Ballester, A, González, F & Muñoz, JA 2009, 'Sugar-beet pulp pectin gels as biosorbent for heavy metals: Preparation and determination of biosorption and desorption characteristics', *Chemical Engineering Journal*, vol. 150, no. 2, pp. 289–301.
39. Mohan, D & Singh, KP 2002, 'Single- and multi-component adsorption of cadmium and Zinc using activated carbon derived from bagasse-an agricultural waste', *Water Research*, vol. 36, no. 9, pp. 2304–2318.
40. Omar, K, Ikram, M, Hamza, L, Mouna, N, Abed, M & Mohamed Lyamine, C 2020, 'Equilibrium, mechanism and mass transfer studies of nickel(II) adsorption by sewage sludge-derived activated carbon', *Iranian Journal of Chemistry and Chemical Engineering*, vol. 40, no. 5, pp. 1675–1682.
41. Özcan, S, Çelebi, H & Özcan, Z 2018, 'Removal of heavy metals from simulated water by using eggshell powder', *Desalination and Water Treatment*, vol. 127, pp. 75–82.
42. Pal, DB, Selvasembian, R & Singh, P 2021, 'Cadmium removal by composite copper oxide/ceria adsorbent from synthetic wastewater', *Biomass Conversion and Biorefinery*, vol. 55, no. 7, pp. 1816–1824.
43. Park, JH, Ok, YS, Kim, SH, Cho, JS, Heo, JS, Delaune, RD & Seo, DC 2016, 'Competitive adsorption of heavy metals onto sesame straw biochar in aqueous solutions', *Chemosphere*, vol. 142, pp. 77–83.
44. Rao, M, Parwate, AV & Bhole, AG 2002, 'Removal of Cr⁶⁺ and Ni²⁺ from aqueous solution using bagasse and fly ash', *Waste Management*, vol. 22, no. 7, pp. 821–830.
45. Reddad, Z, Gerente, C, Andres, Y & Le Cloirec, P 2002, 'Adsorption of Several Metal Ions onto a Low-Cost Biosorbent: Kinetic and Equilibrium Studies', *Environmental Science & Technology*, vol. 36, no. 9, pp. 2067–2073.

46. Schiewer, S & Patil, SB 2008, 'Modeling the effect of pH on biosorption of heavy metals by citrus peels', *Journal of Hazardous Materials*, vol. 157, no. 1, pp. 8–17.
47. Seki, K, Saito, N & Aoyama, M 1997, 'Removal of heavy metal ions from solutions by coniferous barks', *Wood Science and Technology*, vol. 31, no. 6, pp. 441–447.
48. Shukla, SR & Pai, RS 2005, 'Adsorption of Cu(II), Ni(II) and Zn(II) on dye loaded groundnut shells and sawdust', *Separation and Purification Technology*, vol. 43, no. 1, pp. 1–8.
49. Trinelli, MA, Areco, MM & dos Santos Afonso, M 2013, 'Co-biosorption of copper and glyphosate by *Ulva lactuca*', *Colloids and Surfaces B: Biointerfaces*, vol. 105, pp. 251–258.
50. Vázquez, G, Antorrena, G, González, J & Doval, MD 1994, 'Adsorption of heavy metal ions by chemically modified *Pinus pinaster* bark', *Bioresource Technology*, vol. 48, no. 3, pp. 251–255.
51. Venkatraman, Y & Priya, AK 2021, 'Removal of heavy metal ion concentrations from the wastewater using tobacco leaves coated with iron oxide nanoparticles', *International Journal of Environmental Science and Technology*, pp. 1–16.
52. Vijayaraghavan, J, Bhagavathi Pushpa, T, Sardhar Basha, SJ & Jegan, J 2015, 'Isotherm, Kinetic and mechanistic studies of methylene blue biosorption onto red seaweed *Gelidium corticata*', *Desalination and Water Treatment*, vol. 57, no. 29, pp. 13540–13548.
53. Vijayaraghavan, K & Jegan, J 2015, 'Entrapment of brown seaweeds (*Turbinaria conoides* and *Sargassum Wightii*) in polysulfone matrices for the removal of praseodymium ions from aqueous solutions', *Journal of Rare Earths*, vol. 33, no. 11, pp. 1196–1203.
54. Vijayaraghavan, K, Rangabhashiyam, S, Ashokkumar, T & Arockiaraj, J 2017, 'Assessment of samarium biosorption from aqueous solution by brown macroalga *Turbinaria conoides*', *Journal of the Taiwan Institute of Chemical Engineers*, vol. 74, pp. 113–120.
55. Viraraghavan, T & Dronamraju, MM 1993, 'Removal of copper, nickel and Zinc from wastewater by adsorption using feat. *Journal of Environmental Science and Health*', Part A: *Environmental Science and Engineering and Toxicology*, vol. 28, no. 6, pp. 1261–1276